Dielectric-Loaded Plasmonic Switching Elements and Circuits

A. Pitilakis, O. Tsilipakos, and E. E. Kriezis
Department of Electrical and Computer Engineering, Aristotle University of Thessaloniki, GR-54124, Greece
E-mails: alexpiti@auth.gr, otsilipa@auth.gr, mkriezis@auth.gr

***Abstract*- We provide a thorough theoretical investigation of switching elements made of dielectric-loaded surface plasmon polariton waveguides that can meet the practical requirements of board-to-board multi-wavelength optical interconnects. For this purpose, advanced numerical techniques including the finite element method (FEM) and the beam propagation method (BPM) have been employed.**

I. Introduction

Guided wave plasmonics provide a possible route towards nanophotonic circuits with sub-wavelength confinement. Over the last years there has been an abundance of new ideas in this area, mainly along the lines of different waveguiding structures and passive components, backed by strong theoretical investigations and experimental evidence. However, there seems to be a shortage of plasmonic switching elements that can provide the performance anticipated in real-world optical interconnect applications, such as adequate extinction ratio (ER), tolerable insertion losses (IL) and acceptable switching speed. This is the main objective of this study. The underlying guiding structure in the switching elements to be investigated is the Dielectric-Loaded Surface Plasmon Polariton (DLSPP) waveguide [1], which, apart from being technologically simple, provides a good balance between losses and confinement and further allows wave control by tuning the properties of the loading material, most commonly by the thermo-optic effect. We will examine switching elements based on (a) waveguide microring resonators (WRR) and (b) Multi-Mode Interference (MMI) couplers.

II. Microring Based Switching Elements

A typical microring resonator switch consists of a single ring coupled above and below to two parallel (straight) waveguides. Equal coupling gaps implement a 2×2 switch, whereas dissimilar gaps result in a 1×2 switch. Varying the temperature shifts the resonances and hence provides the two states of the switch by changing the preferred output port (through and drop). The performance of such a switch made of DLSPP (typical propagation length $L_{\text{prop}} = 50\,\mu\text{m}$ for PMMA loading) is inherently limited, with the bottleneck being the drop port which suffers a very poor extinction ratio ($\text{ER} < 3\,\text{dB}$) and heavy insertion losses ($\text{IL} > 10\,\text{dB}$). The reason behind these poor figures is the fact that the drop port transmission is not a result of interference; on the contrary, the through port transmission is the resultant of interfering waves and for critical coupling conditions the performance is satisfactory ($\text{ER} > 10\,\text{dB}, \text{IL} < 5\,\text{dB}$).

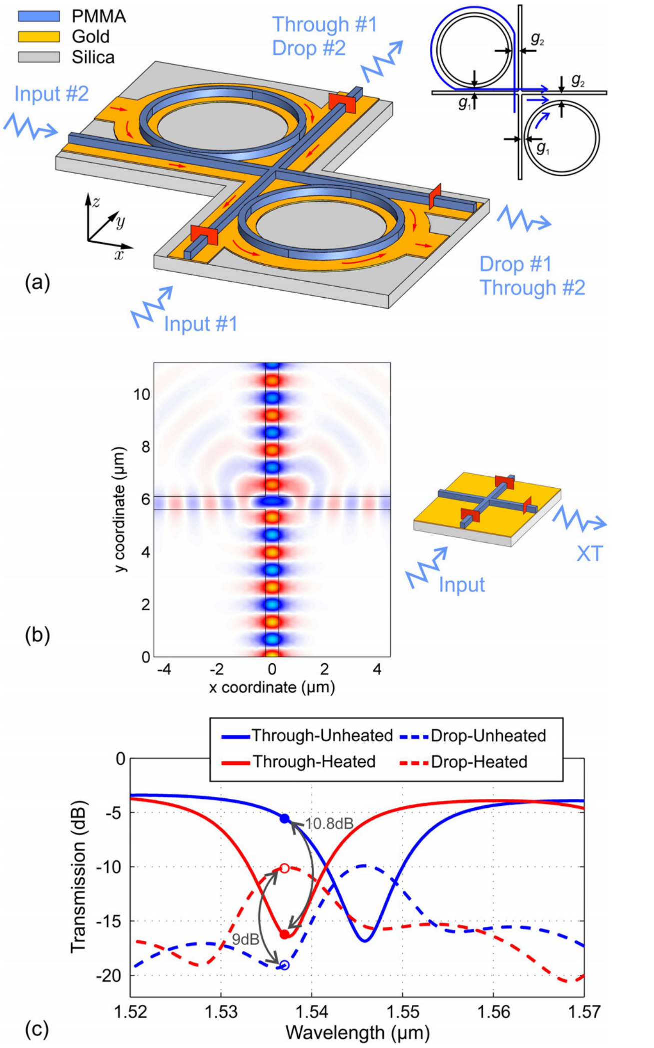

Figure 1. (a) Dual-microring switching element with perpendicular access waveguides. The inset shows the three interfering waves at the drop port: usual drop route, Q-route and XT. (b) Electric field at the waveguide crossing showing the crosstalk. (c) Transmission versus wavelength in the unheated and heated states and for both ports. R=5.5μm, g_1=0.3μm, g_2=0.5μm. Waveguide cross section is 500×600 nm^2 and made of PMMA, metal stripe is 3μm wide and ΔT=100K.

The above facts suggest that in order to improve the drop port ER one has to provide an interference mechanism, and this can be done by introducing a second ring, as in Fig. 1(a). This will provide a second route ("Q" route) and in addition, the waveguide crossing will further contribute with a third

978-1-61284-318-6/11/$26.00 ©2011 IEEE

interfering wave (crosstalk, XT). The amplitude of the XT wave is non-negligible (~ 0.2), as inferred from the FEM analysis of the isolated waveguide crossing depicted in Fig. 1(b) which reveals an XT value of $\sim -15\,\mathrm{dB}$. The proposed switching element has been thoroughly analyzed in the context of vectorial 3D FEM calculations, using prismatic elements. Particular details on the numerical implementation have been reported in [2,3]. The port transmittances versus wavelength are provided in Fig. 1(c); the irregular shape of drop port transmittance confirms the presence of interfering waves as suggested above. It is important to observe the substantial improvement in ER, with the through and drop ports demonstrating an ER of $10.8\,\mathrm{dB}$ and $9\,\mathrm{dB}$, respectively, at the marked wavelength ($1537\ \mathrm{nm}$). In addition, an ER exceeding $8\,\mathrm{dB}$ is sustained in a wavelength window of $3.2\,\mathrm{nm}$ which can accommodate four 100-GHz-spaced WDM channels.

III. Multi-Mode Interference Switching Elements

An alternative approach for constructing a 2×2 switch exploits the beating between two modes in a longitudinal configuration, such as the MMI coupler shown in Fig. 2(a). The MMI section is restricted to a width that supports only two modes: the fundamental TM_{00} mode which has a symmetric E_y component and the TE_{00} mode which has an anti-symmetric E_y. A geometrical dispersion diagram (real part of n_{eff} and L_{prop}) is shown in Fig. 2(b) for both the heated and unheated states. Changing the temperature results in a modification of the phase constants and for sufficient propagation length (L_{MMI}) exchanges the output ports. The inherent losses of the plasmonic modes limit the switch performance in two ways: (a) insertion losses increase with the necessary length L_{MMI} for achieving phase inversion and (b) the different level of losses experienced by the TM_{00} and TE_{00} modes tends to limit the ER and beyond some point, further approaching L_{MMI} is detrimental to the ER. A key element is the design of the input coupler in order to excite both modes at equal proportions. For this class of longitudinal structures with a well defined propagation axis, we are basing our analysis on a finite element beam propagation method (FE-BPM), which is combined with a Padé wide-angle extension [3]. This computational technique ensures fine resolution in the device cross-section, natural treatment of the large jumps in material properties at metal/loading interface and correct capturing of the longitudinally varying sections (input/output couplers). Fig. 2(c) shows the evolution of the extinction ratio along the propagation direction and the interplay between the phase accumulation effect (which tends to increase ER) and the unbalanced level of losses between modes (which tends to suppress ER). Careful design of all parameters can lead to an ER of $17\,\mathrm{dB}$ at an IL level of $12\,\mathrm{dB}$.

Acknowledgment

This work was supported by the European FP7 project PLATON and the HERACLITUS II research fellowship.

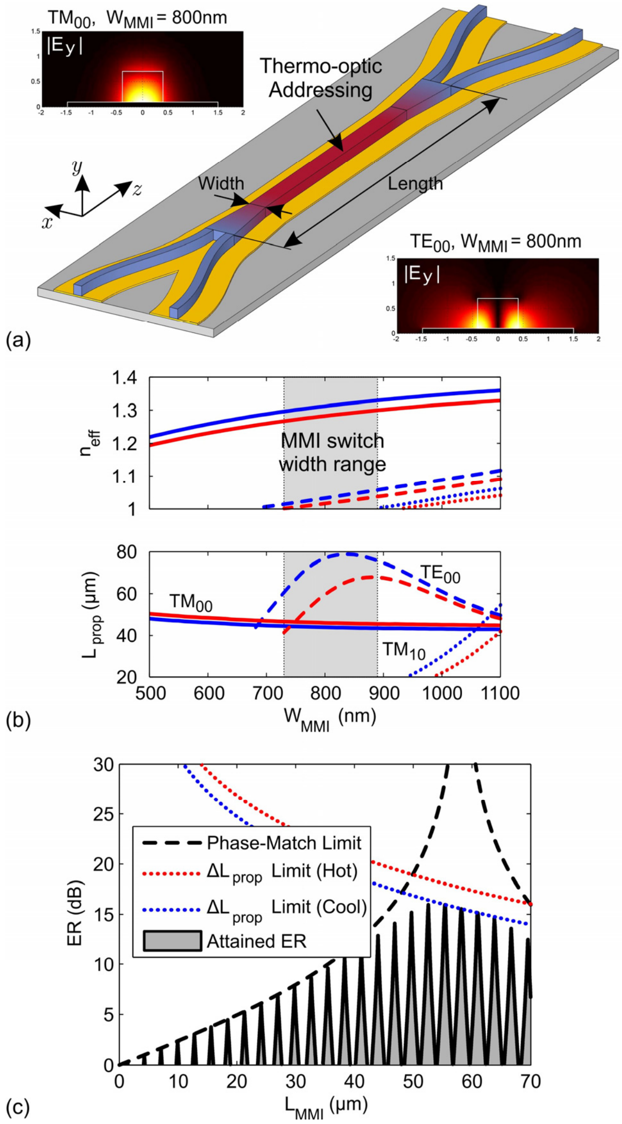

Figure 2. (a) MMI-based switching element. (b) Geometrical dispersion diagram. Gray region indicates the targeted MMI-section width. (c) ER evolution along the device length showing also the limiting bounds due to phase accumulation (dashed black) and the differential losses between TM00 and TE00 in hot (red dotted) and cold (blue dotted) states. ER stays always below the lowest of the three limiting factors. W_{MMI}=$800\ \mathrm{nm}$, feeding waveguides are $500{\times}600\ \mathrm{nm}^2$ and made of a polymer with TOC = $-3\times10^{-4}\ \mathrm{K}^{-1}$, ΔT=100K.

References

[1] T. Holmgaard and S. I. Bozhevolnyi, "Theoretical analysis of dielectric-loaded surface plasmon-polariton waveguides," *Phys. Rev. B*, vol. 75, 245405, 2007.

[2] O. Tsilipakos, T. V. Yioultsis, and E. E. Kriezis, "Theoretical analysis of thermally tunable microring resonator filters made of dielectric-loaded plasmonic waveguides," *J. Appl. Phys.*, vol. 106, 093109, 2009.

[3] O. Tsilipakos, A. Pitilakis, A. C. Tasolamprou, T.V. Yioultsis, E. E. Kriezis, "Computational techniques for the analysis and design of dielectric-loaded plasmonic circuitry," *Opt. Quant. Electron.*, in press.